Biomolecule–nanoparticle hybrids as functional units for nanobiotechnology

Ronan Baron, Bilha Willner and Itamar Willner*

Received (in Cambridge, UK) 25th July 2006, Accepted 15th August 2006
First published as an Advance Article on the web 15th September 2006
DOI: 10.1039/b610721b

Biomolecule–metal or semiconductor nanoparticle (NP) hybrid systems combine the recognition and catalytic properties of biomolecules with the unique electronic and optical properties of NPs. This enables the application of the hybrid systems in developing new electronic and optical biosensors, to synthesize nanowires and nanocircuits, and to fabricate new devices. Metal NPs are employed as nano-connectors that activate redox enzymes, and they act as electrical or optical labels for biorecognition events. Similarly, semiconductor NPs act as optical probes for biorecognition processes. Double-stranded DNA or protein chains that are modified with metallic nanoclusters act as templates for the synthesis of metallic nanowires. The nanowires are used as building blocks to assemble nano-devices such as a transistor or a nanotransporter.

Institute of Chemistry, The Hebrew University of Jerusalem, Jerusalem, 91904, Israel. E-mail: willnea@vms.huji.ac.il; Fax: 972-2-6527715; Tel: 972-2-6585272

Ronan Baron

Dr Ronan Baron acts as a postdoctoral fellow in the laboratory of Prof. I. Willner. He completed his PhD studies at the ENSC Rennes, France in 2002. His research interests include electrochemistry, photoelectrochemistry, synthesis and applications of nanoparticles and the development of molecular and biomolecular switches and logic gates.

The unique electronic, optical, and catalytic properties of metal or semiconductor nanoparticles provide new functional materials that may be integrated with biomolecules. The fact that biomolecules such as enzymes, antigens or DNA exhibit dimensions comparable to those of nanoparticles (NPs) suggest that biomolecule–NP hybrid systems may represent new materials revealing combined and synergistic properties originating from the hybrid composite. These might include the activation of the electronic, optical or catalytic functions of the NPs by biomolecule recognition events or biocatalytic functions of the biomolecules, or, alternatively, the NPs may stimulate and activate the biomolecules. Indeed, substantial progress was accomplished in the last decade in the synthesis and applications of biomolecule–NP hybrid systems, and we are witnessing a recent explosion of diverse research activities that established the mature scientific discipline of nanobiotechnology. Several comprehensive review articles have summarized the advances in the field, and addressed the potential applications of the different systems.[1,2] The present article

Bilha Willner

Dr Bilha Willner acts as a Senior Research Associate in the laboratory of Prof. I. Willner. She completed her PhD studies at the Hebrew University of Jerusalem in 1982 in the area of organometallic chemistry. Her interests include bioelectrochemistry and biosensor design.

Itamar Willner

Prof. Itamar Willner completed his PhD studies in Chemistry in 1978 at The Hebrew University of Jerusalem. After a postdoctoral stay with M. Calvin at the University of California, Berkeley, he joined the Institute of Chemistry at The Hebrew University of Jerusalem in 1982. In 1986 he was appointed Professor at The Hebrew University. He co-authored 450 research papers and acts as a member of several editorial boards. He is the recipient of the Kolthoff Award, The Max-Planck Research Award for International Cooperation, the Israel Chemical Society Award (2001) and the Israel Prize in Chemistry (2002). He is a member of the Israel Academy of Sciences and a member of the European Academy of Sciences and Arts. His research interests include molecular electronics and optoelectronics, nanotechnology, bioelectronics and biosensors, optobioelectronics, nanobiotechnology, supramolecular chemistry, nanoscale chemistry, and monolayer and thin-film assemblies, light-induced electron-transfer processes and artificial photosynthesis.

aims to introduce the topic by discussing several examples, and particularly, some recent advances, while addressing the diverse potential applications of biomolecule–NPs hybrid systems as sensors, nanocircuitry, and for the fabrication of nano-devices.

Redox enzymes usually lack direct electron transfer communication with electrodes due to spatial separation of their redox center from the conductive surface by means of the protein shell.[3] The nanometric dimensions of metal nanoparticles or carbon nanotubes allowed to implant these conducting nano-elements as electrical connectors between the enzyme active site and the electrodes. Au nanoparticles (Au NPs, 1.4 nm) functionalized with a single *N*-hydroxysuccinimide functionality were modified with the aminflavin adenine dinucleotide cofactor, **1**, and linked to the electrode surface by different dithiols, **2–4**, acting as bridges. The apoglucose oxidase, generated by exclusion of its native FAD cofactors, was reconstituted on the cofactor-modified Au NPs (Fig. 1). The reconstitution of the biocatalyst aligned the enzyme and its redox center in a proximal configuration to the Au NPs that mediated the electron transfer to the electrode and activated the bioelectrocatalytic functions of the enzyme.[4] Knowing the surface coverage of the reconstituted enzyme on the electrode and the maximum saturation values of the biocatalytic anodic currents generated in the systems with the different dithiol spacers, **2–4**, the turnover rate constant for transferring the electrons from the active site to the electrode were evaluated. For the dithiol (**2**) the electron transfer turnover rate was estimated to be 5×10^3 s^{-1}, a value that is *ca.* 8-fold higher than the turnover rate of electrons from the cofactor in the native enzyme to its natural acceptor, oxygen (*ca.* 700 s^{-1}). This unprecedented effective electrical contacting of the enzyme with the electrode not only leads to sensitive amperometric biosensors, but to the very selective enzyme electrodes that are unperturbed by the non-catalytic electrochemical oxidation of interfering reagents to glucose analysis such as ascorbic acid or uric acid. The effectiveness of the electrochemical wiring of glucose oxidase by the Au NPs was found to be controlled by the dithiol bridges, **2** > **3** > **4**. While the fully conjugated bridge **2** led to the most efficient electron transfer communication the tilting of the adjacent biphenyl rings in **3** and the existence of two sp^3 barriers in **4** decreased the electron tunneling, respectively. Similarly, the electrical contacting of other redox proteins such as the pyrroloquinoline quinone-dependent glucose dehydrogenase was accomplished by the reconstitution of the apo-enzyme on the cofactor-functionalized Au NPs.[5] Also, the reconstitution of apo-glucose oxidase on other nano-elements such as FAD-functionalized carbon nanotubes led to effective electrical wiring of the proteins with electrode supports.[6] The effective electron transfer communication of redox enzymes with electrodes by means of conductive nano-objects is invaluable for the future development of amperometric biosensors and biofuel cell elements.[7]

Metallic or semiconductor NPs may also be employed as tags for the electrochemical detection of biorecognition events.[8,9] For example,[10] different metal sulfide NPs, *i.e.*, ZnS, CdS and PbS functionalized with different probe nucleic

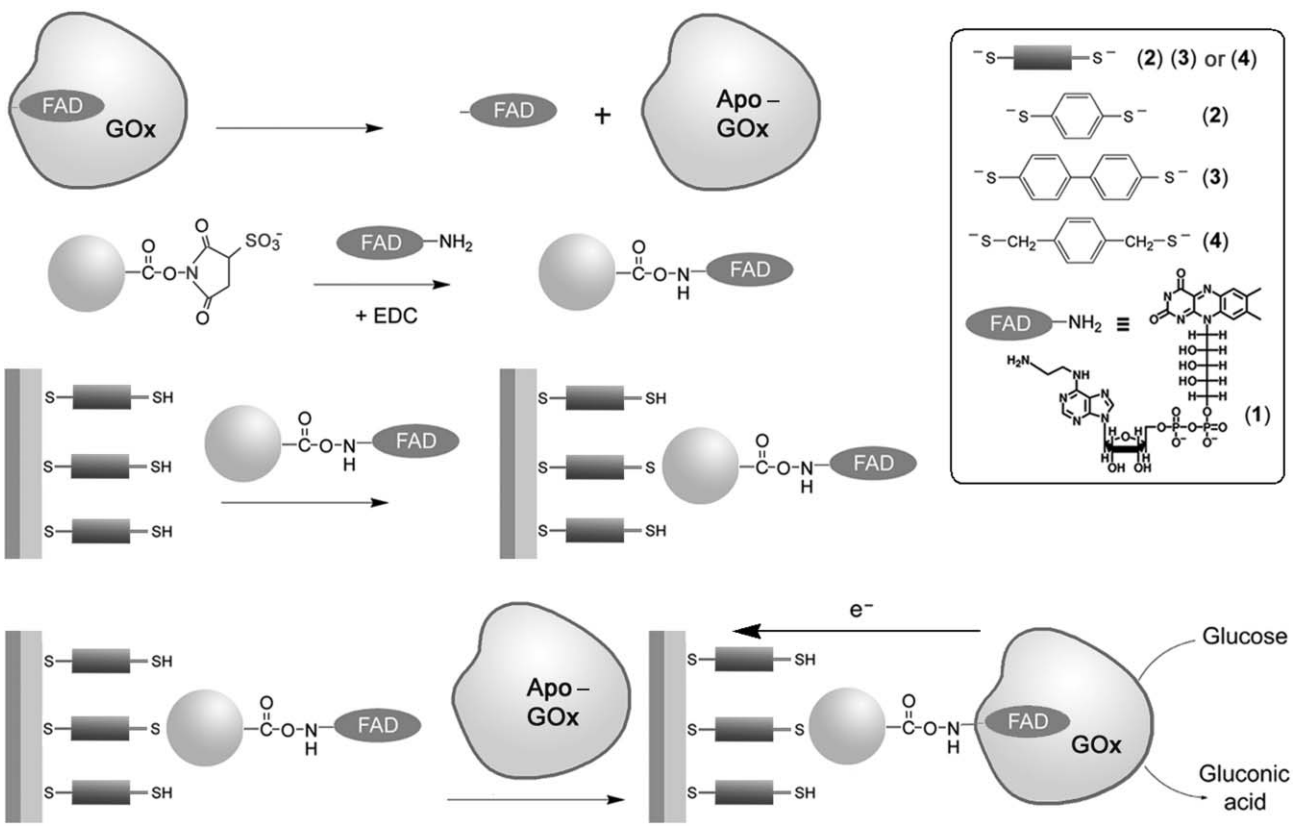

Fig. 1 Assembly of a Au NP-reconstituted GOx electrode.

acids were used as codes for the simultaneous analysis of three different 60-mer DNA targets related to the breast cancer gene, BRCA1 (Fig. 2(A)). Magnetic particles were functionalized with three different nucleic acids, **5–7**, that are complementary to parts of the three different target DNA. Hybridization with one (or all targets, a, b, c) leads to the formation of the respective duplexes. Metal sulfide-functionalized NPs that include each of the nucleic acids complementary to each of the targets, **8–10**, act as tracers that follow the hybridization of the targets. The metal sulfide NPs hybridize with the DNA assemblies associated with the magnetic particles, provided that the target(s) hybridize with sensing nucleic acids (in the specific example shown in Fig. 2(A) all targets exist in the sample, and thus all three nucleic acid-functionalized metal sulfide tracers bind to the magnetic particles). The subsequent magnetic separation of the magnetic particles, followed by the dissolution of the metal sulfide NPs enabled the parallel and simultaneous analysis of the different targets. The analysis of the dissolved ions by stripping voltammetry led to well separated voltammograms that corresponded to the different targets (Fig. 2(B)). The current responses provided a quantitative measure for the concentrations of the different targets. By the use of other metal sulfides such as GaS or InS and the further incorporation of metal NPs, *e.g.*, Au, Ag, Pd NPs, the diversity of parallel sensing may be further improved. This method was further extended to analyze proteins by aptamer-functionalized surfaces, using metal sulfide-functionalized proteins as tracers for the proteins.[11]

Metal nanoparticles and semiconductor quantum dots (QDs) exhibit unique optical properties controlled by their sizes. Indeed, metal NPs and semiconductor QDs were extensively used as optical reporters for biorecognition events.[12] Biomolecularly induced aggregation (or deaggregation) of metal NP clusters, or biocatalytic transformations on the NPs or QDs that control the optical properties of the particles pave the way, however, to new exciting opportunities in nanobiotechnology. The aggregation of Au NPs leads to a coupled interparticle plasmon absorbance giving rise to red-shifted exciton corresponding to the aggregated cluster.[13] This leads to a blue color of clustered Au NPs as compared to the red color characteristic to individual, separated, Au NPs. The clustering of Au NPs and the accompanying red to blue color transitions were used to analyze DNA[14] (Fig. 3). Au NPs were

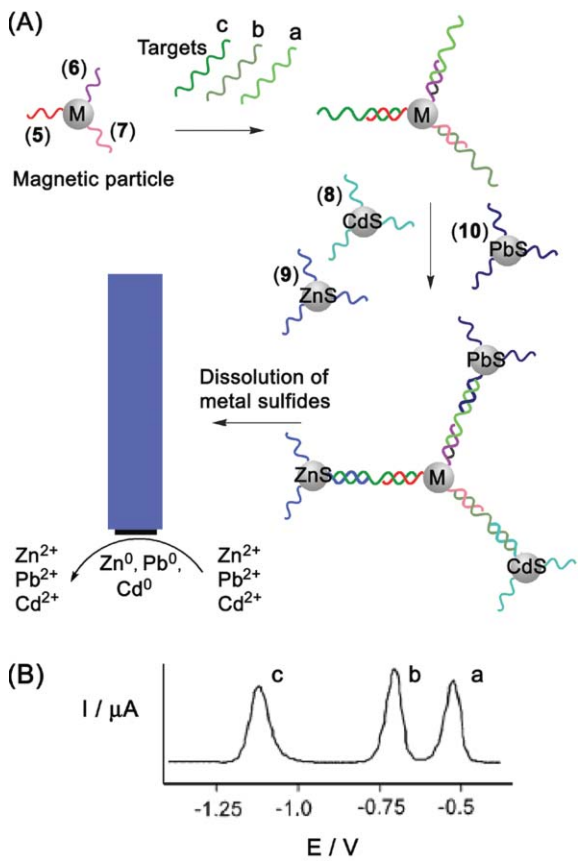

Fig. 2 (A) Multi-target electrochemical detection of DNA by metal sulfide nanoparticles tracers. (B) Typical stripping voltammograms for the metal tracers upon analysis of three different DNAs, 54 nM. Peaks correspond to (a) PbS, (b) CdS, (c) ZnS. (Fig. 2(B) is reprinted from ref. 10*a*, with permission; Copyright American Chemical Society, 2003.)

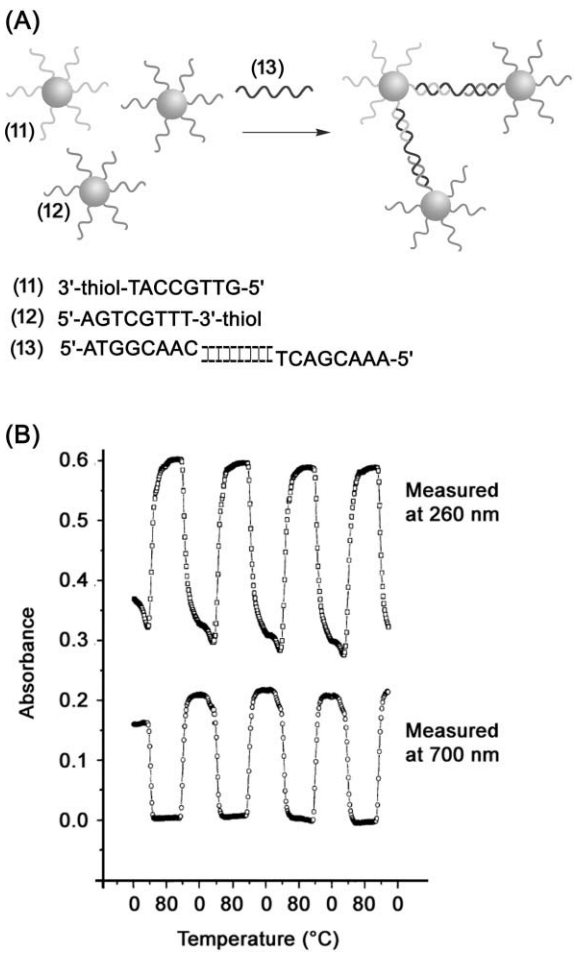

Fig. 3 (A) Schematic representation of the aggregation of DNA-functionalized Au NPs through the hybridization with an analyte DNA. (B) Absorbance versus temperature/time for DNA/colloid hybridized materials. (Fig. 3(B) is reprinted from ref. 14, with permission; Copyright Nature Publishing Group, 1996.)

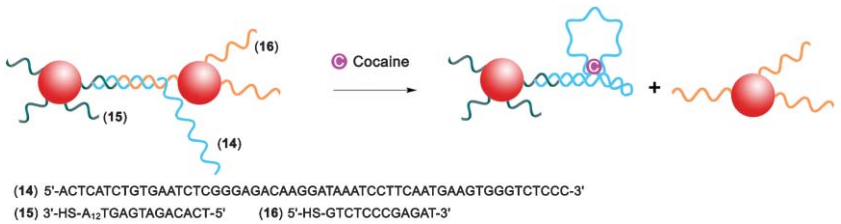

Fig. 4 Colorimetric detection of cocaine by the cocaine-induced dissociation of Au aggregated nanoparticles crosslinked by a cocaine aptamer.

modified with nucleic acids **11** and **12**, complementary to the ends of the analyzed DNA (**13**). The hybridization of the analyte with the modified Au NPs results in their bridging and aggregation. Typical colorimetric transitions upon the DNA-stimulated aggregation of the NPs are depicted in Fig. 3(B). The hybridization efficiency and the melting temperatures of the resulting duplex aggregates were found to be controlled by the existence of mutations,[15a] and by the sizes of the Au NPs.[15b] This enabled the development of rapid colorimetric methods for DNA analysis with the ability to detect single base mismatches in the analyzed strands.

The optical monitoring of biorecognition processes through the separation of Au NP aggregates is exemplified by the colorimetric detection of cocaine by its specific aptamer.[16] The aptamer against cocaine was elongated by a nucleic acid sequence that forms the structure **14** (Fig. 4). Au NPs functionalized with two nucleic acids **15** and **16** that are complementary to parts of **14**, are used as optical reporter units for cocaine. The hybridization of the **15**- and **16**-modified Au NPs leads to the aggregation of the particles and the appearance of the blue color. Treatment of the aggregate with cocaine results in the folding of the aptamer to the cocaine-binding configuration, a process that leads to the separation of the Au NPs. The dissociation of Au NP aggregates for colorimetric sensing was similarly applied for the analysis of Pb^{2+} ions by the cooperative biocatalyzed cleavage of a nucleic acid-crosslinked Au NP aggregate by a Pb^{2+}-dependent DNAzyme.[17]

The biocatalyzed synthesis of metallic NPs allowed the optical assaying of enzymes, and the development of different colorimetric detection schemes for biocatalytic transformations.[18] For example, tyrosinase is a Cu^{2+}-dependent enzyme that hydroxylates phenol residues (such as tyrosine) to the respective catechol products (*e.g.* L-DOPA). Elevated concentrations of tyrosinase are found in melanoma cancer cells, and tyrosinase is considered as biomarker of these cells.[19] The reduction of $AuCl_4^-$ to Au NPs by the L-DOPA product generated by the tyrosinase-mediated oxidation of tyrosine by O_2 was used to assay tyrosinase[20] (Fig. 5). As the content of tyrosinase increases, the concentration and sizes of the biocatalytically synthesized Au NPs increase. Other enzymes were similarly used to grow metallic NPs, and to develop colorimetric detection schemes for the respective substrates of the enzymes. The biocatalytically generated H_2O_2 by flavoenzymes such as glucose oxidase,[21] or the 1,4-dihydronicotinamide adenine dinucleotide (phosphate), NAD(P)H, generated by different $NAD(P)^+$-dependent enzymes such as lactate dehydrogenase or alcohol dehydrogenase,[22] acted as reducing agents for the reduction of $AuCl_4^-$ on Au NP catalytic seeds. Similarly, the alkaline phosphatase mediated the hydrolysis of *p*-aminophenol phosphate to *p*-aminophenol that reduced Ag^+-ions on Au NP seeds.[23] The catalytic enlargement of the metal NPs enabled the optical detection of the substrates that corresponded to the respective enzymes, by following the plasmon absorbance features of the synthesized metal NPs.

The unique optical properties of semiconductor nanoparticles (quantum dots, QDs) that reveal size-controlled luminescence properties, impressive photostability, and high quantum yields provide further opportunities to apply these materials for biosensing.[24] Indeed, substantial research efforts were directed to the use of semiconductor QDs as fluorescence labels, that substitute conventional organic dyes or transition metal complexes, for the imaging of biorecognition events.[12] The potential of semiconductor QDs rests, however, on the possibility to perform chemical reactions on biomolecule-functionalized surfaces, thus enabling the photonic imaging of biorecognition or biocatalytic processes occurring on the QDs.

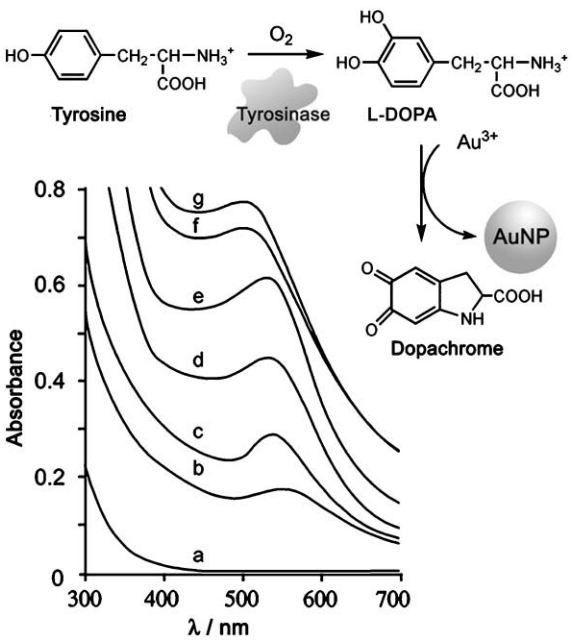

Fig. 5 (A) Assay of tyrosinase activity through the biocatalyzed oxidation of tyrosine and the L-DOPA-mediated formation of Au NPs. (B) Absorbance spectra of Au NPs formed by variable concentrations of tyrosinase: (a) 0 U ml^{-1}, (b) 10 U ml^{-1}, (c) 20 U ml^{-1}, (d) 30 U ml^{-1}, (e) 35 U ml^{-1}, (f) 40 U ml^{-1}, (g) 60 U ml^{-1}. The system includes tyrosine, 2×10^{-4} M, $HAuCl_4$, 2×10^{-4} M, CTAC, 2×10^{-3} M, in 0.01 M PB. Spectra were recorded after a fixed time interval of 10 min. (Adapted from ref. 20, with permission; Copyright American Chemical Society, 2005.)

Furthermore, the size-controlled optical properties of QDs enable the multiplexed, parallel, analysis of several targets with labels of identical composition but different sizes. The use of semiconductor QDs for biosensing is exemplified here with the assay of telomerase. Telomerase is a ribonucleoprotein that elongates the chromosomal telomer units and transforms them into immortal cells. Thus, telomerase is a versatile marker for cancer cells, and over 95% of different cancerous cells reveal elevated amounts of telomerase.[25] CdSe/ZnS core shell QDs were modified with the thiolated nucleic acid **17** that is recognized by telomerase. In the presence of the nucleotides mixture, dNTPs, the Texas-Red-labeled dUTP, and telomerase extracted from HeLa cancer cells, telomerization of the nucleic acid **17** was initiated in a similar path that proceeds on the ends of the chromosomes.[26] The telomerization results in the incorporation of the Texas-Red (TR) units into the telomers, and the activation of the fluorescence resonance energy transfer (FRET) from the QDs to the dye labels (Fig. 6). The fluorescence generated by the dye was then used to follow the activity of the telomerase.

A further example that utilized a biomolecule-semiconductor QDs conjugate for sensing involves the optical detection of the explosive trinitrotoluene, TNT (**18**).[27] CdSe–ZnS core–shell QDs were functionalized with the trinitrobenzene recognizing antibody (Fig. 7(A)). The azobenzene dye tethered to the trinitrobenzene antigen **19** was bound to the antibodies associated with the QDs, and it quenched the fluorescence of the QDs. In the presence of the TNT analyte the quencher was

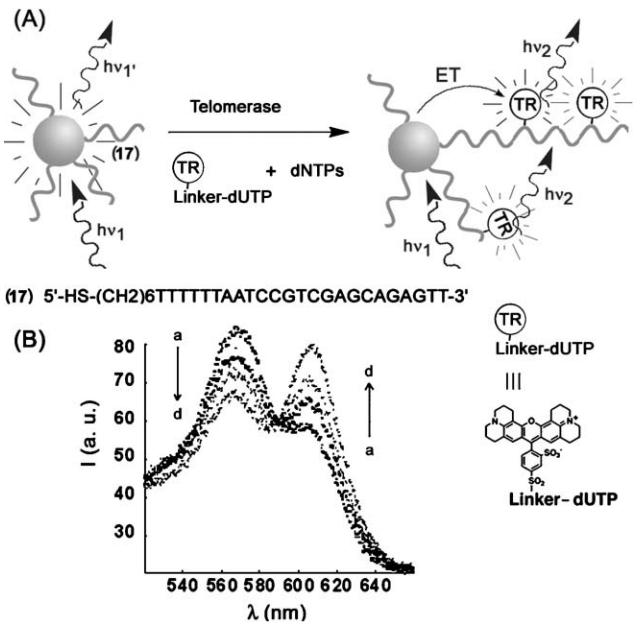

Fig. 6 (A) Telomerization on the **17**-functionalized CdSe–ZnS QDs with the incorporation of Texas red-labeled dUTP. (B) Time-dependent emission spectra upon telomerization on the CdSe–ZnS QDs: (a) before addition of telomerase; (b), (c) and (d), after 10, 30 and 60 min of telomerization, respectively, in the presence of telomerase (extracted from HeLa cells, 10 000 cells) and a mixture of dNTPs (dATP, dCTP and dGTP, 0.5 mM each) and **6** (100 μM). (Fig. 6(B) is adapted from ref. 26, with permission; Copyright American Chemical Society, 2003.)

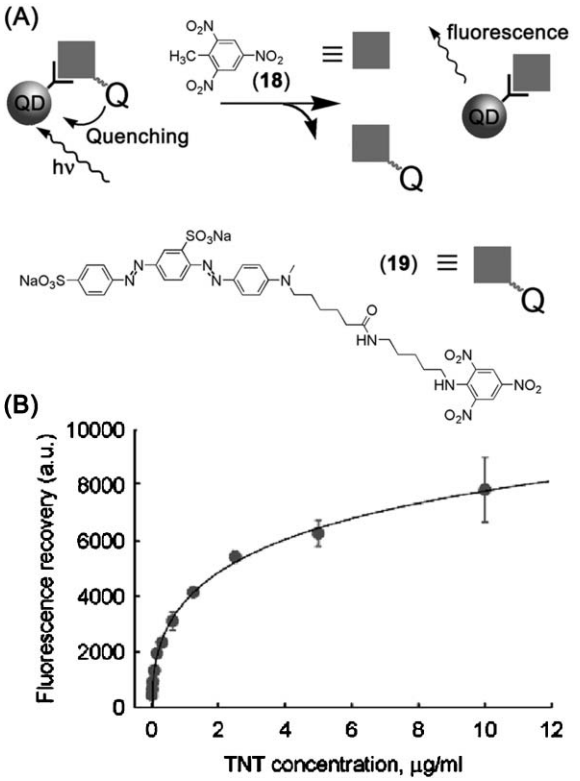

Fig. 7 (A) Optical analysis of the trinitrotoluene (TNT) by a competitive immunoassay that involves the fluorescence quenching of the QDs by a quencher-TNT analog. (B) Calibration curve corresponding to the fluorescence of the QD/**19** system upon analyzing different concentrations of TNT (**18**). (Fig. 7(B) is adapted from ref. 27, with permission; Copyright American Chemical Society, 2005.)

competitively displaced, and the fluorescence of the QDs was restored. As the concentration of the explosive increased, the fluorescence of the QDs was enhanced (Fig. 7(B)).

The past fifty years have demonstrated a revolution in microelectronics reflected with the immense miniaturization of electronic and computing devices. The lithographic methods to miniaturize electronic circuitries are probably reaching their limits, and the development of alternative approaches is a challenging goal in modern science. The ''bottom-up'' approach, where functional nanometer-sized objects are constructed by the assembly of molecules or polymers that act as templates for the synthesis of nanocircuitry is one of the promising perspectives of nanotechnology.[28] Albeit the ''bottom-up'' approach is not free of limitations, and fundamental issues, such as the high throughput synthesis of the nano-objects, or the fabrication of defect-free devices, need to be resolved, the topic reveals extraordinary challenges and attracts substantial research efforts.

The properties and functions of DNA suggest that it might be a useful template for the synthesis of nanocircuitry.[28] The ease to synthesize DNA of controlled lengths and various shapes, together with the information stored in the base sequence introduce rich structural properties and addressability for the direction of chemical components to dictated domains. Also, the variety of enzymes that catalyze different transformations on DNA, such as ligase (ligation), polymerase

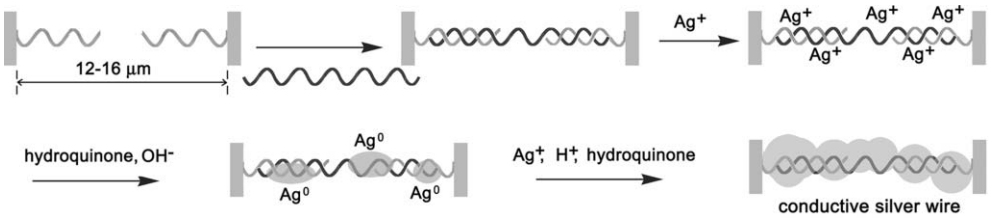

Fig. 8 The construction of a Ag^0 nanowire bridging two microelectrodes.

(replication), telomerase (elongation) or endonucleases (scission), provide unique biocatalytic nano-tools to manipulate the DNA templates. In addition, the association of metal ions to the phosphate groups or the intercalation of molecules in between bases or minor/major grooves of the duplex DNA enables the targeting of ions to the template, and the initiation of chemical transformations that yield the nanowires.

The use of the DNA as a template for the generation of Ag^0 nanowires is depicted[29] in Fig. 8. The 12–16 nm gap between two microelectrodes was bridged by a nucleic acid by attaching its two ends to complementary thiolated nucleic acids associated with the microelectrodes. Ion exchange of the phosphate counter ions, followed by the hydroquinone-induced reduction of the ions resulted in silver nanoclusters associated with the DNA wire template. The subsequent catalytic enlargement of the Ag^0 nanoclusters using an acidic Ag^+/hydroquinone solution resulted in the formation of continuous Ag^0 nanowires that were *ca.* 100 nm wide. Related methods were applied to synthesize other metal nanowires such as Pt,[30] Pd[31] or Cu.[32] Also, intercalator-modified Au NPs were self-assembled on DNA templates through the inter-base association of the intercalator units.[33] Semiconductor NPs[34] or organic conducting polymers[35] (*e.g.*, polyaniline) were similarly assembled on DNA templates, thus demonstrating that different nanowire composites may be synthesized on the DNA templates.

The sequence-specific winding of a homologous nucleic acid carried by the RecA protein was used to address the nucleic acid/protein complex on the DNA scaffold. The metallization of the free, non-protein-coated, DNA segments enabled then the sequence-specific molecular lithography of the DNA-based nanowires.[36] This approach for the molecular nanolithography patterning of DNA templates was used to fabricate nano-transistors based on DNA templates (Fig. 9(A)). A single

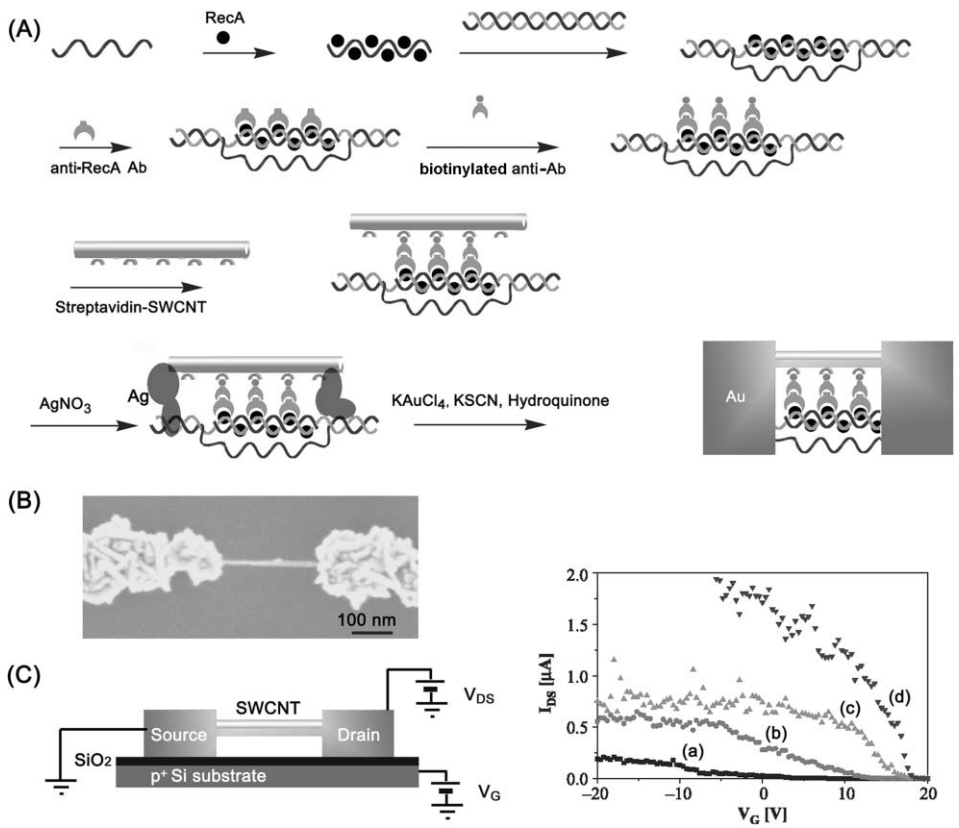

Fig. 9 (A) The construction of a DNA-templated SWCNT FET. (B) SEM image of a rope of SWCNTs and metallic wires contacting it. (C) Electrical circuit and electrical characterisation of the DNA-templated SWCNT FET. The drain-source current is given versus gate voltage for different values of drain-source bias, (a) VDS = 0.5 V, (b) 1 V, (c) 1.5 V, (d) 2 V. (Fig. 9(B) and 9(C) are reprinted from ref. 36, with permission; Copyright AAAS, 2003.)

stranded nucleic acid sequence was complexed with RecA and carried to a double-stranded duplex DNA, a process that led to the nanolithographic patterned insulation of the DNA template by the protein. A carbon nanotube was then specifically attached to the protein patch using a series of antigen–antibody recognition processes. The anti-RecA antibody was bound to the protein linked to the DNA duplex, and the biotinylated anti-antibody was then linked to the RecA-Ab. The latter Ab was used to specifically bind the streptavidin-coated carbon nanotubes. The subsequent reduction of the Ag^+-exchanged DNA duplex segments to Ag^0 nanoclusters, followed by the catalytic electroless enlargement of the Ag^0 nanoclusters with gold, generated the device where the two Au contacts were bridged by the carbon nanotubes. A representative SEM image of the device is depicted in Fig. 9(B). The resulting device deposited on a Si substrate acted as a field-effect nano-transistor, where the gold contacts bridged by the CNT acted as the nanoscale source and drain electrodes, and the current flow through the CNT was gated by the applied potential on the Si support (Fig. 9(C)).

Proteins may similarly act as templates to synthesize nanowires, and might even reveal some superior properties for the generation of nanocircuitry. The fact that proteins reveal specific binding and catalytic functions (*e.g.*, enzymes) might lead to the formation of biocatalytic templates that self-synthesize functional nanocircuitry. Also, different proteins exhibit motor functions, and reveal motility on surfaces. The use of motor proteins as templates for the synthesis of nanowires may yield chemically triggered transportable nanocircuitry that could be positioned at desired locations by their motility along patterned tracks on surfaces. These functions of proteins, together with the rich available chemistry to modify proteins and to immobilize them on surfaces provide invaluable features for the ''bottom-up'' synthesis of nanostructures on protein templates. Indeed, different metallic[37] or semiconductor[38] nanowires were synthesized on protein templates. Also, synthetic peptides were successfully applied as templates for the directed assembly of nanoparticles.[39]

The F-actin/myosin proteins couple acts as an ATP-driven motor protein assembly.[40] Au nanowires with motility functions were synthesized on the actin template.[41] G-Actin monomer units were modified with single Au nanoparticles (1.4 nm). The monomers were then polymerized, and the Au-NPs were enlarged by chemical means to form a continuous Au nanowire (Fig. 10(A)). Fig. 10(B) shows a typical AFM image of the resulting nanowire that exhibited a height of *ca.* 80–100 nm and lengths that were in the range of 1–2 μm. Conductivity measurements revealed that the conductivity features of the resulting nanowires were similar to those of bulk gold. The nanowires that exhibit motility functions were synthesized by the primary polymerization of the Au

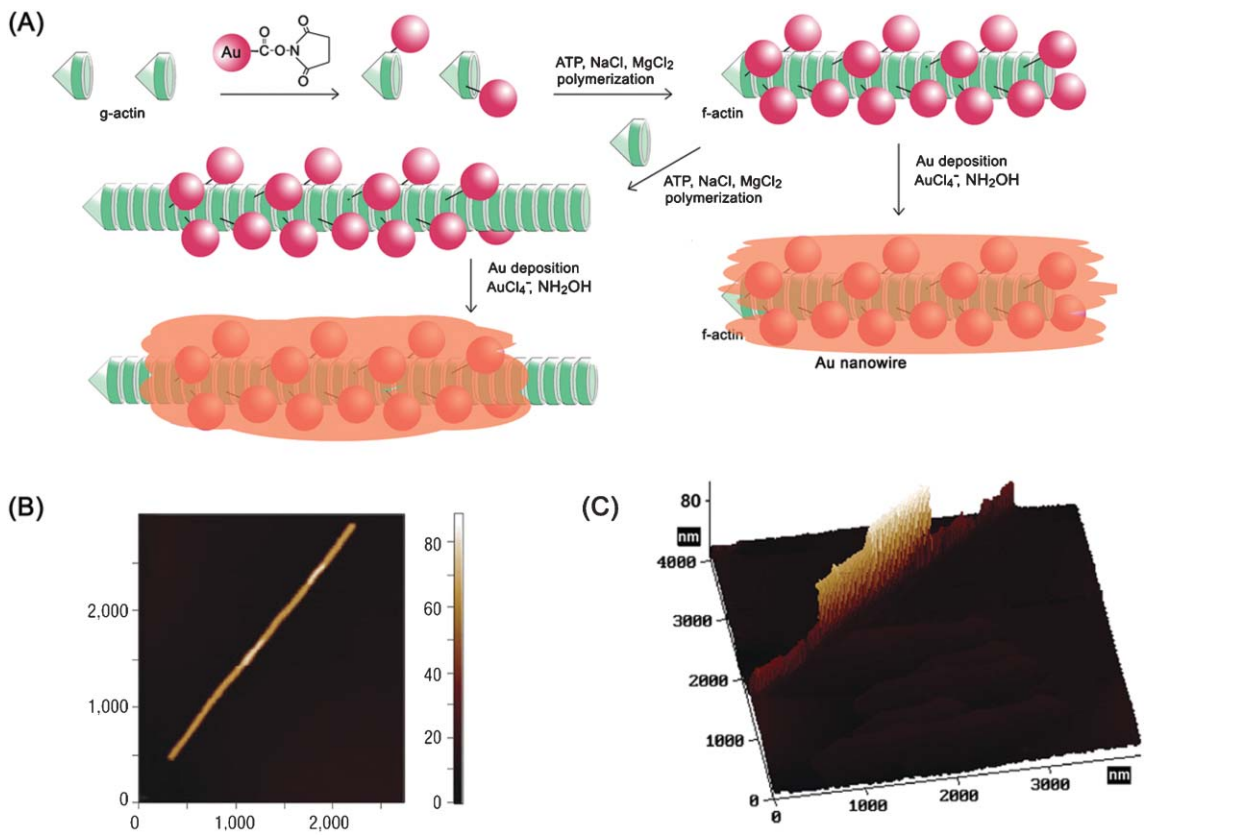

Fig. 10 (A) The synthesis of an Au nanowire on an F-actin template and the synthesis of an Au nanowire linked to F-actin filaments. (B) AFM image of an Au nanowire generated on an actin template. (C) AFM image of the resulting actin/Au wire/actin filament nanostructure. All dimensions in (B) and (C) are in nanometers. (Fig. 10(B) and 10(C) are adapted from ref. 41, with permission; Copyright Nature Publishing Group, 2004.)

NP-functionalized G-actin units followed by the polymerization of unmodified G-actin monomers with the ends of the Au nanoparticle-modified filaments (Fig. 10(A)). The chemical catalytic reduction of $AuCl_4^-$ resulted in the enlargement of the filament modified with the Au NPs, thus leading to the formation of a Au nanowire that includes at its ends two base actin filaments (Fig. 10(C)). The actin/Au-nanowire/actin nanostructure revealed motor functions. The motility of the nanostructure on a surface functionalized with myosin was triggered by the addition of the ATP fuel substrate, and microscopy images indicated that the nanostructures moved on the surface at a rate corresponding to 250 ± 50 nm s^{-1}. Besides the possibility to dynamically address these actin-functionalized metallic nanowires to dictated locations on surfaces, one might consider the further applications of these functional nanostructures as transporters that carry "chemical cargos" on the Au nanowire support.

A different approach to generate nanowires has involved the use of "biocatalytic inks" as active templates for the synthesis of nanostructures.[23] Different enzymes catalyze the formation of products that reduce metal salts to metals on appropriate catalytic metallic seeds. For example, flavin-based oxidases generate upon the oxidation of the respective substrates H_2O_2, and this acted as a reducing agent of $AuCl_4^-$ in the presence of Au seeds.[21] Similarly, nicotinamide adenine dinucleotide (NAD^+)-dependent enzymes yield, in the presence of the respective substrates, the reducing agent 1,4-dihydronicotinamide adenine dinucleotide (NADH). This reducing agent mediated the catalyzed reduction of $AuCl_4^-$ on Au NPs, a process that resulted in the enlargement of the nanoparticles.[22] This enabled the use of Au-NP-functionalized enzymes as "biocatalytic inks" for the dip-pen nanolithographic patterning of the biocatalytic templates on surfaces (*e.g.*, Si support). The subsequent biocatalytic enlargement of the catalytic seeds associated with the templates resulted in the formation of continuous nanowires. Fig. 11(A) exemplifies the concept by depositing Au NP-functionalized glucose oxidase as template for the growth of Au nanowires. The biocatalytic oxidation of glucose by oxygen yielded H_2O_2, and the latter product reduced $AuCl_4^-$ and enlarged the NPs to a contacted continuous metallic Au nanowires (Fig. 11(B)). The width and height of the nanowires were in the range of 120–150 nm, and the growth process was blocked at these dimensions. Other metal nanowires could be similarly synthesized by other biocatalytic inks. For example, the Au NP-functionalized alkaline phosphatase hydrolyzed *p*-aminophenol phosphate, and the hydroquinone-type product reduced Ag^+ ions on the Au NPs and led to the formation of Ag^0 nanowire with characteristic width/height dimensions of 25–50 nm (Fig. 11(C)). By the dip-pen nanolithographic deposition of different "biocatalytic inks" on surfaces, templates that allowed the orthogonal synthesis of different metal NPs were prepared. Nanopatterns of Au NP-functionalized glucose oxidase and Au NP-modified alkaline phosphatase were deposited on the Si surfaces, and the orthogonal stepwise synthesis of Au nanowires and Ag nanowires was accomplished by the reaction of the surface alternatively with glucose and *p*-aminophenol phosphate, (**20**, respectively, Fig. 11(D). An important feature of the biocatalytic growth of metallic nanowires, that highlights the advantage of this metal growth mechanism over the chemical electroless metal deposition reactions, is the fact that the biocatalyzed synthesis of the

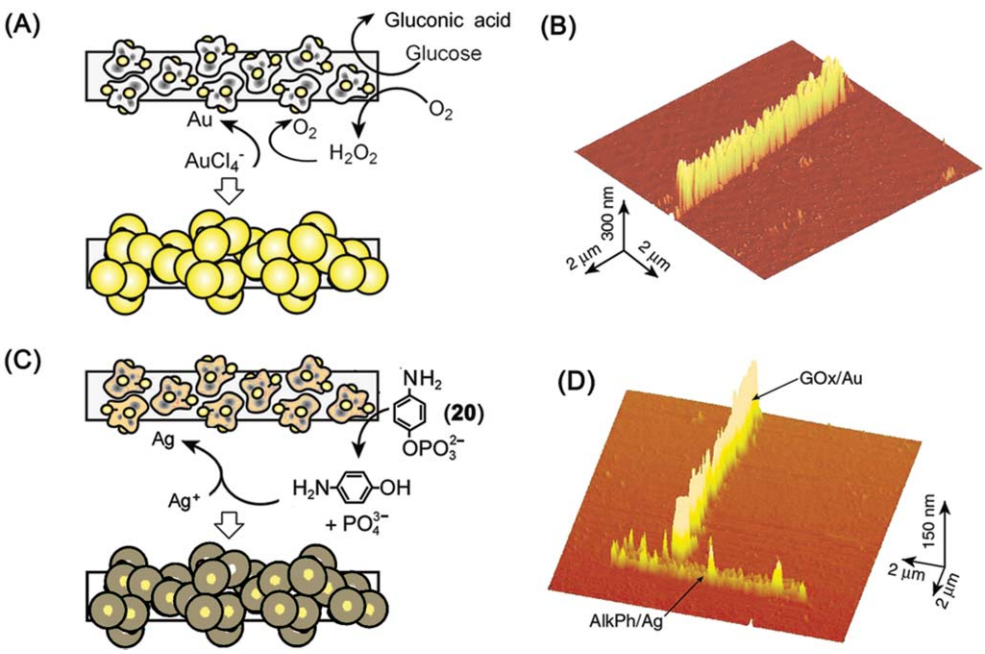

Fig. 11 (A) The generation of a Au nanowire by the biocatalytic enlargement of a Au NP-functionalized GOx line deposited on a silicon support by dip-pen nanolithography (DPN). (B) AFM-image of the Au nanowire generated by the Au NP-functionalized GOx as "biocatalytic ink". (C) Application of the Au NPs-functionalized alkaline phosphatase as biocatalytic ink for the synthesis of an Ag nanowire. (D) AFM-image of Au and Ag nanowires generated by deposition and enlargement of the Au NP/GOx template and the subsequent deposition of Au NP/AlkPh template and its enlargement to the Ag nanowire. (Adapted from ref. 23, with permission; Copyright Wiley-VCH, 2006.)

nanowires includes a self-inhibiting mechanism that becomes significant as the nanowires are enlarged. That is, the growth of the particles reveals a saturation kinetics, and the biocatalytic enlargement of the nanowires is terminated when the biocatalyst is coated by the metal shell and diffusion of the substrate to the active site is blocked.

The present article has featured some recent advances in the area of nanobiotechnology. The unique tailored functions of biomolecule/NP or biomolecule/quantum dot hybrid systems were already established, and their application for the development of biosensors, nanocircuitry and devices was demonstrated. The future perspectives of the field are bright and promising. The rapid progress in the synthesis of nanoparticles of unique shapes and structures, such as tripod or tetrapod nanoparticles,[42] core-shell[43] or hollow metal NPs[44] and the elucidation of the unique optical properties of these structures pave the way for new labeling materials for sensing. Another challenging research direction involves the use of biomolecules as active components for the assembly and functional triggering of nanoscale structures. Substantial recent efforts that are directed to utilize biomolecules, particularly DNA, as building block units for the autonomous self-assembly of nanostructures[45] or as functional units that duplicate and mimic machine-like functions,[46] open the way to integrate NPs with these ingenious biomolecular nanostructures and to design new materials of tailored properties and functions. The controlled aggregation of NPs or the development of biocatalytic transformations for the repair of NPs aggregates[47] are just simple examples for the future potential of such systems. Also, the progress of the microelectronic industry to fabricate nanometer-sized gaps between electrodes opens new opportunities to couple biomolecular nanostructures within these gaps, and to assemble new biosensors or nanoscale devices. For example, the deposition of biomolecule–NP conjugates within the gap of microelectrodes as a result of a biorecognition event might provide a useful concept to assemble sensing arrays and to readout the recognition events by impedance measurements. Similarly, the biomolecule–NP conjugate bound to the nano-sized gap separating the microelectrodes could be employed as a functional building block unit and semiconductor insulator, or metallic nanostructures may be biocatalytically addressed to the gap and yield nano-devices. The rapid progress in nanobiotechnology promises exciting future opportunities where chemists, physicists, biologists and material scientists will find a rich playground of challenging interdisciplinary activities.

Acknowledgements

Our research on nanobiotechnology is supported by The German–Israeli Research Program (DIP), The Israel Ministry of Science and The Johnson & Johnson Corporation.

References

1 E. Katz and I. Willner, *Angew. Chem., Int. Ed.*, 2004, **43**, 6042.
2 (*a*) C. M. Niemeyer, *Angew. Chem., Int. Ed.*, 2001, **40**, 4128; (*b*) H. Gu, K. Xu, C. Xu and B. Xu, *Chem. Commun.*, 2006, 941.
3 (*a*) A. Heller, *Acc. Chem. Res.*, 1990, **23**, 128; (*b*) A. Heller, *J. Phys. Chem.*, 1992, **96**, 3579; (*c*) I. Willner, E. Katz and B. Willner, *Electroanalysis*, 1997, **9**, 965; (*d*) I. Willner and E. Katz, *Angew. Chem., Int. Ed.*, 2000, **39**, 1180; (*e*) I. Willner, *Science*, 2002, **298**, 2407.
4 Y. Xiao, F. Patolsky, E. Katz, J. F. Hainfeld and I. Willner, *Science*, 2003, **299**, 1877.
5 M. Zayats, E. Katz, R. Baron and I. Willner, *J. Am. Chem. Soc.*, 2005, **127**, 12400.
6 F. Patolsky, Y. Weizmann and I. Willner, *Angew. Chem., Int. Ed.*, 2004, **43**, 2113.
7 A. Heller, *Phys. Chem. Chem. Phys.*, 2004, **6**, 209.
8 (*a*) E. Katz, I. Willner and J. Wang, *Electroanalysis*, 2004, **16**, 19; (*b*) R. A. Bullen, T. C. Arnot, J. B. Lakeman and F. C. Walsh, *Biosens. Bioelectron.*, 2006, **21**, 2015.
9 (*a*) J. Wang, D. Xu, A.-N. Kawde and R. Polsky, *Anal. Chem.*, 2001, **73**, 5576; (*b*) J. Wang, R. Polsky and D. Xu, *Langmuir*, 2001, **17**, 5739; (*c*) J. Wang, O. Rincón, R. Polsky and E. Dominguez, *Electrochem. Commun.*, 2003, **5**, 83.
10 (*a*) G. Liu, T. M. H. Lee and J. Wang, *J. Am. Chem. Soc.*, 2005, **127**, 38; (*b*) J. Wang, G. Liu, R. Polsky and A. Merkoçi, *Electrochem. Commun.*, 2002, **4**(2002), 722; (*c*) G. Liu, J. Wang, J. Kim, M. R. Jan and G. E. Collins, *Anal. Chem.*, 2004, **76**, 7126.
11 J. A. Hansen, J. Wang, A. -N. Kawde, Y. Xiang, K. V. Gothelf and G. Collins, *J. Am. Chem. Soc.*, 2006, **128**, 2228.
12 (*a*) I. L. Medintz, H. T. Uyeda, E. R. Goldman and H. Mattoussi, *Nat. Mater.*, 2005, **4**, 435; (*b*) M. Bruchez, Jr., M. Moronne, P. Gin, S. Weiss and A. P. Alivisatos, *Science*, 1998, **281**, 2013; (*c*) X. Y. Wu, H. J. Liu, J. Q. Liu, K. N. Haley, J. A. Treadway, J. P. Larson, N. F. Ge, F. Peale and M. P. Bruchez, *Nat. Biotechnol.*, 2003, **21**, 41.
13 A. N. Shipway, M. Lahav, R. Gabai and I. Willner, *Langmuir*, 2000, **16**, 8789.
14 C. A. Mirkin, R. L. Letsinger, R. C. Mucic and J. J. Storhoff, *Nature*, 1996, **382**, 607.
15 (*a*) G. P. Mitchell, C. A. Mirkin and R. L. Letsinger, *J. Am. Chem. Soc.*, 1999, **121**, 8122; (*b*) J. -S. Lee, S. I. Stoeva and C. A. Mirkin, *J. Am. Chem. Soc.*, 2006, **128**, 8899.
16 J. Liu and Y. Lu, *Angew. Chem., Int. Ed.*, 2006, **45**, 90.
17 (*a*) J. Liu and Y. Lu, *J. Am. Chem. Soc.*, 2003, **125**, 6642; (*b*) J. Liu and Y. Lu, *Anal. Chem.*, 2004, **76**, 1627.
18 I. Willner, R. Baron and B. Willner, *Adv. Mater.*, 2006, **18**, 1109.
19 C. Angeletti, V. Khomitch, R. Halaban and D. L. Rimm, *Diagn. Cytopathol.*, 2004, **31**, 33.
20 R. Baron, M. Zayats and I. Willner, *Anal. Chem.*, 2005, **77**, 1566.
21 (*a*) M. Zayats, R. Baron, I. Popov and I. Willner, *Nano Lett.*, 2005, **5**, 21; (*b*) Y. Xiao, V. Pavlov, B. Shlyahovsky and I. Willner, *Chem. Eur. J.*, 2005, **11**, 2698.
22 Y. Xiao, V. Pavlov, S. Levine, T. Niazov, G. Markovitch and I. Willner, *Angew. Chem., Int. Ed.*, 2004, **43**, 4519.
23 B. Basnar, Y. Weizmann, Z. Cheglakov and I. Willner, *Adv. Mater.*, 2006, **18**, 713.
24 (*a*) A. P. Alivisatos, *Nat. Biotechnol.*, 2004, **22**, 47; (*b*) A. P. Alivisatos, *J. Phys. Chem.*, 1996, **100**, 13226.
25 (*a*) C. B. Harley, A. B. Futcher and C. W. Greider, *Nature*, 1990, **345**, 458; (*b*) W. E. Wright, M. A. Piatyszek, W. E. Rainey, W. Byrd and J. W. Shay, *Develop. Genet.*, 1996, **18**, 173.
26 F. Patolsky, R. Gill, Y. Weizmann, T. Mokari, U. Banin and I. Willner, *J. Am. Chem. Soc.*, 2003, **125**, 13918.
27 E. R. Goldman, I. L. Medintz, J. L. Whitley, A. Hayhurst, A. R. Clapp, H. T. Uyeda, J. R. Deschamps, M. E. Lassman and H. Mattoussi, *J. Am. Chem. Soc.*, 2005, **127**, 6744.
28 Q. Gu, C. Cheng, R. Gonela, S. Suryanarayanan, S. Anabathula, K. Dai and D. T. Haynie, *Nanotechnology*, 2006, **17**, R14.
29 E. Braun, Y. Eichen, U. Sivan and G. Ben-Yoseph, *Nature*, 1998, **391**, 775.
30 J. Richter, M. Mertig, W. Pompe, I. Monch and H. K. Schackert, *Appl. Phys. Lett.*, 2001, **78**, 526.
31 M. Mertig, L. C. Ciacchi, R. Seidel, W. Pompe and A. De Vita, *Nano Lett.*, 2002, **2**, 841.
32 C. F. Monson and A. T. Woolley, *Nano Lett.*, 2003, **3**, 359.
33 F. Patolsky, Y. Weizmann, O. Lioubashevski and I. Willner, *Angew. Chem., Int. Ed.*, 2002, **41**, 2323.
34 T. Torimoto, M. Yamashita, S. Kuwabata, T. Sakata, H. Mori and H. Yoneyama, *J. Phys. Chem. B*, 1999, **103**, 8799–8803.
35 (*a*) R. Nagarajan, W. Liu, J. Kumar, S. K. Tripathy, F. F. Bruno and L. A. Samuelson, *Macromolecules*, 2001, **34**, 3921; (*b*) Y. Xiao, A. B. Kharitonov, F. Patolsky, Y. Weizmann and I. Willner,

Chem. Commun., 2003, 1540; (*c*) A. Dawn and A. K. Nandi, *Langmuir*, 2006, **22**, 3273.
36 K. Keren, R. S. Berman, E. Buchstab, U. Sivan and E. Braun, *Science*, 2003, **302**, 1380.
37 (*a*) M. Reches and E. Gazit, *Science*, 2003, **300**, 625; (*b*) T. Scheibel, R. Parthasarathy, G. Sawicki, X. M. Lin, H. Jaeger and S. L. Lindquisat, *Proc. Natl. Acad. Sci. USA*, 2003, **100**, 4527.
38 K. K. W. Wong and S. Mann, *Adv. Mater.*, 1996, **8**, 928.
39 (*a*) S. R. Whaley, D. S. English, E. L. Hu, P. F. Barbara and A. M. Belcher, *Nature*, 2000, **405**, 665; (*b*) B. R. Peelle, E. M. Krauland, K. D. Wittrup and A. M. Belcher, *Langmuir*, 2005, **21**, 6929.
40 (*a*) R. D. Vale, *J. Cell Biol.*, 2003, **163**, 445; (*b*) C. G. dos Remedios and P. D. J. Moens, *Biochim. Biophys. Acta*, 1995, **1228**, 99.
41 F. Patolsky, Y. Weizmann and I. Willner, *Nat. Mater.*, 2004, **3**, 692.
42 (*a*) S. H. Chen, Z. L. Wang, J. Ballato, S. H. Foulger and D. L. Carroll, *J. Am. Chem. Soc.*, 2003, **125**, 16186; (*b*) T. K. Sau and C. J. Murphy, *J. Am. Chem. Soc.*, 2004, **126**, 8648; (*c*) Y. Xiao, B. Shlyahovsky, I. Popov, V. Pavlov and I. Willner, *Langmuir*, 2005, **21**, 5659.
43 (*a*) L. Wang, J. Luo, Q. Fan, M. Suzuki, I. S. Suzuki, M. H. Engelhard, Y. Lin, N. Kim, J. Q. Wang and C.-J. Zhong, *J. Phys. Chem. B*, 2005, **109**, 21593; (*b*) Y. Cao, R. Jin and C. A. Mirkin, *J. Am. Chem. Soc.*, 2001, **123**, 7961; (*c*) K. P. Velikov and A. van Blaaderen, *Langmuir*, 2001, **17**, 4779; (*d*) X. Peng, M. C. Schlamp, A. V. Kadavanich and A. P. Alivisatos, *J. Am. Chem. Soc.*, 1997, **119**, 7019.
44 Y. Sun and Y. Xia, *Anal. Chem.*, 2002, **74**, 5297.
45 (*a*) N. C. Seeman, *Trends Biochem. Sci.*, 2005, **30**, 119; (*b*) J. Zheng, P. E. Constantinou, C. Micheel, A. P. Alivisatos, R. A. Kiehl and N. C. Seeman, *Nano Lett.*, 2006, **6**, 1502.
46 Y. Weizmann, Z. Cheglakov, V. Pavlov and I. Willner, *Angew. Chem., Int. Ed.*, 2006, **45**, 2238.
47 J. Liu, D. P. Wernette and Y. Lu, *Angew. Chem., Int. Ed.*, 2005, **44**, 7290.

